Dressed fluxon in a Josephson window junction

Jean Guy Caputo
Laboratoire de Mathématiques, Institut National de Sciences Appliquées, BP8, F-76131 Mont-Saint-Aignan, Cedex, France

Nikos Flytzanis
Physics Department, University of Crete, GR-71409 Iraklion, Crete, Greece

Michel Devoret
Service de Physique de l'Etat Condensé, Commissariat à l'Energie Atomique, Saclay, 91191 Gif-sur-Yvette, France
(Received 6 April 1994)

The static fluxon solutions of a Josephson window junction have been studied numerically. We show that the effect of the idle region surrounding the junction is to "dress" the fluxon causing its energy to increase. This effect can be predicted accurately by a simple model.

A fluxon in a Josephson tunnel junction provides the simplest example of a topological, intrinsically nonlinear excitation in an electromagnetic system. A Josephson tunnel junction consists of two overlapping superconducting thin films, which are separated by a thin oxide layer. This insulating layer forms a potential barrier through which Cooper pairs can tunnel.[1] The electrodynamical state of the junction is characterized by the value of the phase difference $\delta(x,y)$ at every point (x,y) of the barrier, which can be considered as a portion of plane. The phase difference obeys a partial differential equation of the sine-Gordon type.[2] For "large" junctions, i.e., junctions where at least one dimension is much greater than the Josephson penetration length λ_J, it is well known that this equation admits solitonlike solutions, which correspond to flux quanta (fluxons) trapped inside the junction, the flux lines running parallel to the plane of the junction.[3] The static and dynamical properties of these fluxons have been extensively studied both experimentally and theoretically.[3,4] Microwave oscillators based on the shuttle motion of fluxons inside a current-biased junction have been proposed.[4] In this paper we investigate numerically the static shape of a fluxon in a variant type of Josephson tunnel junction, the window junction (see Fig. 1). Window junctions are fabricated by depositing on top of the oxidized bottom film a thick, window-shaped, perfectly insulating layer before depositing finally the counter electrode. Thus, tunneling occurs only between the two portions of the films facing each other in the interior of the insulating window. Window junctions are important from a practical point of view because they have the advantage over ordinary junctions to have a more uniform, better controlled oxide barrier.[5] This occurs because in a window junction the perimeter of the oxide layer does not coincide with the edges of the superconductor films, which are often of poor quality because of the patterning process. Furthermore, the outer slabs of the superconductor can play the role of the cavity[6] and enhance the power of fluxon oscillators.

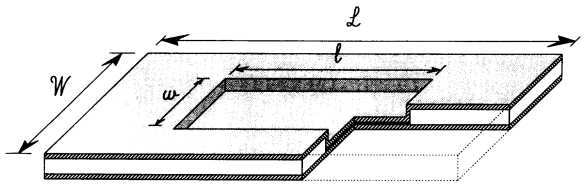

FIG. 1. Cut-away view of a window Josephson junction. Josephson tunneling takes place only inside the window, through a thin oxide layer represented by a thick line. The idle region outside the window confines flux lines entering or leaving the window and tends to increase the magnetic energy of fluxons.

We model the window junction as an array of inductors,[7] whose nodes i are each connected to ground by a Josephson element (see Fig. 2) obeying the Josephson relations. These relations involve the phase difference δ_i across and the current I_i through the Josephson element

$$\dot{\delta}_i = \left[\frac{\hbar}{2e}\right] V_i \ , \tag{1}$$

$$I_i = I_{0i}\sin(\delta_i) \ . \tag{2}$$

Here $V_i(t)$ and I_{0i} denote the voltage and critical current of the junction at node i. Introducing the time integral of the voltage at node i,

$$\Phi_i = \int_{-\infty}^{t} V_i(t')dt' = \left[\frac{\hbar}{2e}\right]\delta_i \ , \tag{3}$$

which has the dimension of a flux, we can write the total energy of the window junction as

$$E = E_m + E_J \ , \tag{4}$$

where

$$E_m = \sum_{\text{nearest neighbors } i,j} \frac{(\Phi_i - \Phi_j)^2}{2L_{ij}} \ , \tag{5}$$

$$E_J = \sum_{\text{junctions } i} I_{0i}\frac{\hbar}{2e}\left[1-\cos\left[\frac{2e}{\hbar}\Phi_i\right]\right] \ . \tag{6}$$

The first term E_m is the magnetic energy of the surface

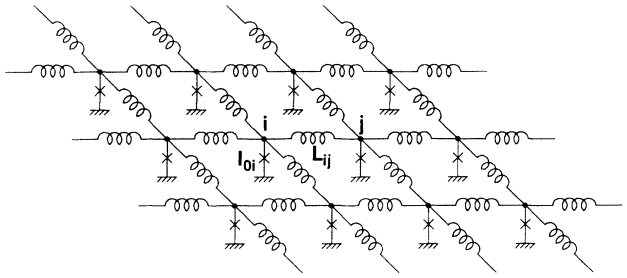

FIG. 2. Portion of equivalent circuit model corresponding to the window junction displayed in Fig. 1. Crosses represent tunnel elements. The critical current I_{0i} is nonzero only inside the window.

currents of the junction induced by the gradient of the phase difference, while the second term E_J is the Josephson energy of Cooper pairs tunneling across the barrier. The symbol L_{ij} stands for the inductance between node i and node j. Only the tunnel region of the junction inside the window contributes to the Josephson energy, since outside, in the idle region, $I_{0i}=0$. On the other hand, both the tunnel region ($\mathcal{T}$) and the idle region ($\mathcal{I}$) contribute to the magnetic energy. If a is the distance between two nodes, the link between this discrete model and the parameters of the window junction is given by the relations

$$L_{ij}=L_J=\mu_0(t_J+\lambda_{1L}+\lambda_{2L}),\quad (i,j)\in\mathcal{T}\ , \tag{7}$$

$$L_{ij}=L_I=\mu_0(t_I+\lambda_{1L}+\lambda_{2L}),\quad (i,j)\in\mathcal{I}\ , \tag{8}$$

$$I_{0i}=\frac{J_0}{a^2}\ , \tag{9}$$

$$\lambda_J=\left[\frac{\hbar}{2e}\frac{1}{L_J J_0}\right]^{1/2}\ , \tag{10}$$

where t_J, t_I, λ_{1L}, λ_{2L}, J_0, and λ_J refer to the tunnel and insulating layer thicknesses, the London penetration lengths of the top and bottom superconducting films, the critical current density of the tunnel barrier and the Josephson length in the tunnel region, respectively. Minimizing formally the energy with respect to the Φ_i's one gets the set of coupled equations

$$\sum_{\text{nearest neighbors } j \text{ of } i}\frac{\Phi_i-\Phi_j}{L_{ij}}+I_{0i}\sin\left[\frac{2e}{\hbar}\Phi_i\right]=0\ , \tag{11}$$

which in the limit $a\to 0$ are equivalent to Maxwell's equations combined with the Josephson relations; these reduce in the static case to

$$\Delta\delta_J=\frac{\sin(\delta_J)}{\lambda_J^2}\ , \tag{12}$$

$$\Delta\delta_I=0\ , \tag{13}$$

where δ_J and δ_I refer to the phase difference field in the junction and in the idle region, respectively. Equations (12) and (13) must be supplemented with the following interface and boundary conditions

$$\delta_J=\delta_I \text{ and } \frac{1}{L_I}\frac{\partial\delta_I}{\partial n}=\frac{1}{L_J}\frac{\partial\delta_J}{\partial n} \tag{14}$$

on the junction interface and

$$\frac{\partial\delta_I}{\partial n}=0 \tag{15}$$

on the idle region boundary. The virtue of the discrete model is that these conditions are automatically satisfied by (11). We have obtained numerically the solution of (11) by minimizing (4) by the conjugate gradient method of Polak and Ribiere.[8] An important feature of the method is that given an initial condition antisymmetrical with respect to the long axis of the junction, the algorithm preserves the antisymmetry at each iteration stage. This is useful, since static solutions in a finite junction are only marginally stable with respect to translation in the absence of magnetic field, which is the case under study here.

Examples of fluxon solution are shown in Fig. 3, for several values of the window width w, the width of the tunnel region. These calculations were done with an idle

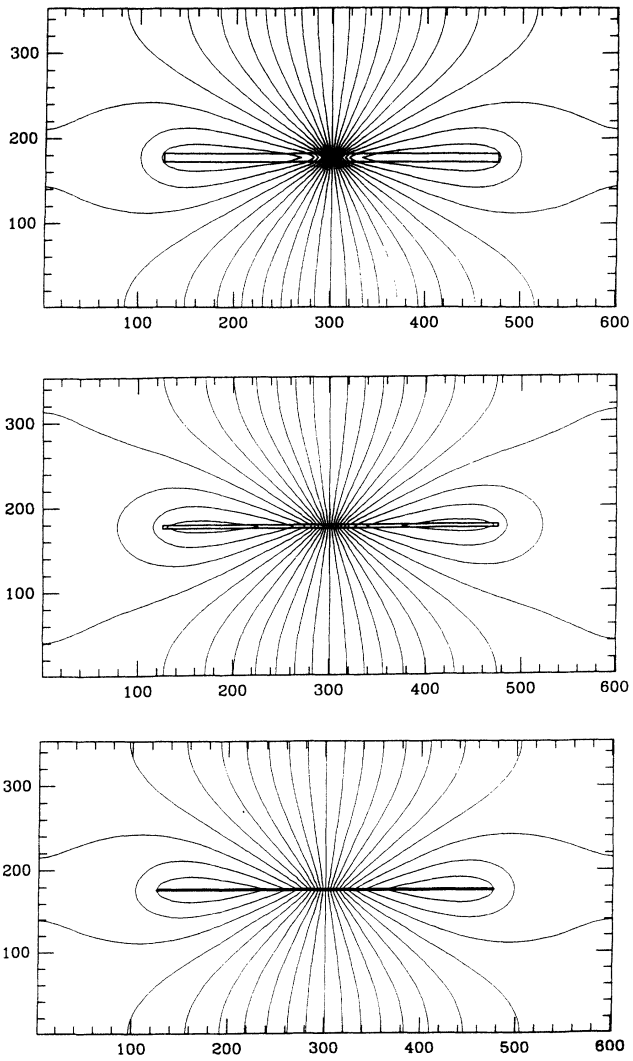

FIG. 3. Contour plots of constant phase difference. In units of the mesh size, the characteristic lengths of the junction are $\lambda_J=5$, $\mathcal{L}=600$, $\mathcal{W}=350$, $l=350$, $w=11$ (top), 5 (middle), and 3 (bottom). There are 23 contour lines, varying between $\delta=\pi/12$ and $23(\pi/12)$. The inflation of the fluxon as w decreases is clearly visible.

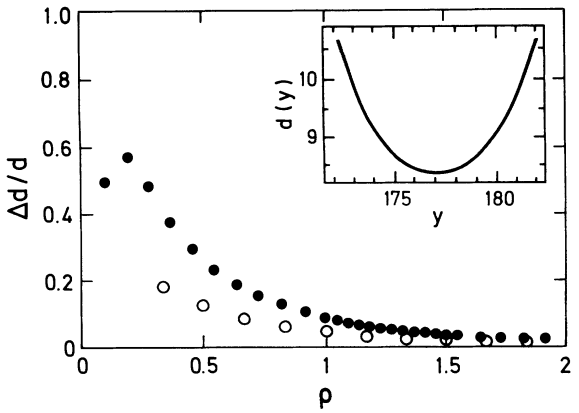

FIG. 4. Plot of $\Delta d/d=[d(y_{\max})-d(y_{\text{center}})]/d(y_{\text{center}})$ as a function of $\rho=\lambda_J/w$ for fixed values of l and w corresponding to the top (black dots) and bottom (white dots) contour plots of Fig. 3. See text for the precise definition of the fluxon width $d(y)$. The line $y=y_{\text{center}}$ is the horizontal symmetry axis of the junction. The inset shows $d(y)$ for the top plot of Fig. 3.

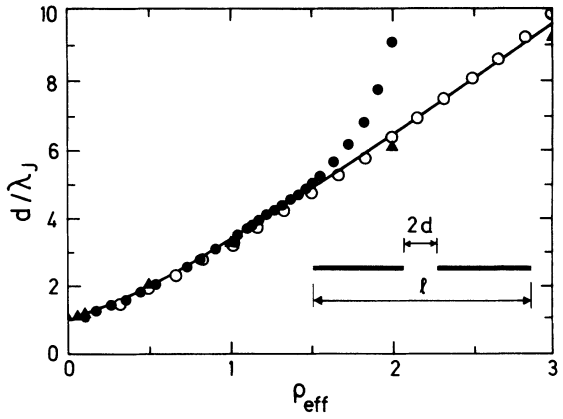

FIG. 5. Plot of the reduced fluxon width d/λ_J as a function of $\rho_{\text{eff}}=\rho L_J/L_I$. The white and black dots correspond to the two sets of data presented in Fig. 4 ($L_J=L_I$, varying λ_J). Dark triangles correspond to the geometry corresponding to the middle contour plot of Fig. 3 with $\lambda_J=5$, L_J/L_I varying between 5×10^{-3} and 3. The inset shows the infinitely thin 2D capacitator whose electrostatic energy can be used to estimate the magnetic energy of the idle region of the window junction.

region sufficiently large so that finite-size effects were negligible. A remarkable effect is that the fluxon width increases when w decreases. The cause of the effect is the interaction of the fluxon inside the tunnel region with the idle region, which tries to decrease the fluxon magnetic energy. The situation is similar to that of a charged particle, which becomes dressed when it is inside a polarizable medium. In order to investigate quantitatively this dressing effect we define the fluxon width by the following procedure.

For an infinitely long tunnel junction with no idle region, the analytic expression

$$\delta(x,y)=4\tan^{-1}(e^{-x/d(y)}) \tag{16}$$

is a solution of (12), provided that the parameter $d(y)$ coincides for every y with λ_J. We have found that our numerical solutions of (11) can be well fitted inside the tunnel region by an expression of the form of (16). For values of $\rho=\lambda_J/w$ large compared to 1, the limit of interest here, we have found that $d(y)$ is approximately equal to a constant d as seen in Fig. 4. In the limit $\rho\gg1$ where inflation occurs, the fluxon can thus conveniently be characterized by this parameter d alone. In Fig. 5 we plot the variations of the parameter d characterizing our numerical results as a function of $\rho_{\text{eff}}=\rho(L_J/L_I)$. We have found empirically that the dependence of the inflation ratio d/λ_J on ρ_{eff} can be remarkably well described by the functional form

$$\frac{d}{\lambda_J}=\frac{\pi}{2}\rho_{\text{eff}}(1+\sqrt{1+4/\pi^2\rho_{\text{eff}}^2}) , \tag{17}$$

for several values of the ratio L_I/L_J. This function plotted as a continuous line in Fig. 5 is a simple interpolation between $d/\lambda_J\approx\pi\rho_{\text{eff}}$ for large ρ_{eff} and $d/\lambda_J\approx1$ for small ρ_{eff}. This behavior can be understood as follows. Consider a window junction with an infinite idle region. One can define the one-parameter class of function $\delta_d(x,y)$ such that (i) inside the tunnel region $\delta_d(x,y)$ is given by (16) with $d(y)=d$, (ii) $\delta_d(x,y)$ satisfies the Laplace equation in the idle region. The magnetic and Josephson energy can be computed exactly inside the tunnel junction. One finds

$$E_m^J=\frac{4w}{dL_J} , \tag{18}$$

$$E_J^J=\frac{4dw}{\lambda_J^2L_J} . \tag{19}$$

In the idle region one can evaluate the magnetic energy by considering that the solution is well approximated by the 2D potential field produced by two colinear segments of total length l at potential 0 and 2π separated by $2d$ (see inset in Fig. 5). One finds, for $l\gg2d$

$$E_m^I=\frac{4\pi}{L_I}=\ln\left[\frac{l}{2d}\right] . \tag{20}$$

Summing the contributions (18), (19), and (20) and minimizing with respect to d, one obtains exactly the simple expression (17). This "inflation" is also present for smaller idle regions, where expression (17) provides an upper bound for the fluxon width. The details of the calculations will be presented in a forthcoming publication.

In conclusion, this work has shown that a fluxon in a window junction becomes "dressed" with the magnetic energy in the idle region. This effect manifests itself by an inflation of the fluxon, which for a long junction is given by (17) to a very good approximation. An important consequence of this inflation of the dressed fluxon is that it carries relatively more energy than the bare fluxon and is therefore of interest in fluxon oscillators, where

this energy is released when the fluxon collides at the junction end.

This work is partially supported by the EEC Project No. SC1*-0229C and the Greek-French collaboration agreement. J.G.C. is thankful for the hospitality of the University of Crete. The authors acknowledge discussions with D. Estève, J. C. Fernandez, G. Reinisch, and C. Roblin.

[1]B. D. Josephson, in *Superconductivity,* edited by A. Parks (Marcel Dekker, New York, 1969).

[2]A. C. Scott, F. Y. Chu, and S. A. Reible, J. Appl. Phys. **47**, 3272 (1976).

[3]A. Barone and G. Paterno, *Physics and Applications of the Josephson Effect* (Wiley Interscience, New York, 1982).

[4]*Stimulated Effects in Josephson Devices,* edited by M. Russo and G. Costabile (World Scientific, Singapore, 1990).

[5]J. M. Pritchard and W. H. Schroen, IEEE Trans. Magn. **MAG-4**, 320 (1968).

[6]A. Larsen, H. Dalsgaard Jensen, and J. Mygind, Phys. Rev. B **43**, 10 179 (1991).

[7]K. K. Likharev, *Dynamics of Josephson Junctions and Circuits* (Gordon and Breach, New York, 1986), Chap. 13.

[8]W. H. Press, B. P. Flannery, S. A. Teukolsky, and W. T. Vetterling, *Numerical Recipes: the Art of Scientific Computing* (Cambridge University Press, Cambridge, England, 1986).

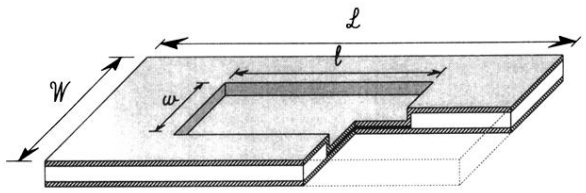

FIG. 1. Cut-away view of a window Josephson junction. Josephson tunneling takes place only inside the window, through a thin oxide layer represented by a thick line. The idle region outside the window confines flux lines entering or leaving the window and tends to increase the magnetic energy of fluxons.